Particle Size and Morphological Evaluation of Airborne Urban Dust Particles by Scanning Electron Microscopy and Bidimensional Empirical Mode Analysis

MARCELA MORVIDONE[1], IVANA MASCI[2], DIANA RUBIO[1], MELISA KURTZ[2],
DEBORAH TASAT[2] AND ROSA PIOTRKOWSKI[1]
[1]Centro de Matemática Aplicada,
Instituto de Tecnologías Emergentes y Ciencias Aplicadas (ITECA) UNSAM-CONICET,
25 de Mayo y Francia, B1650 San Martin, Buenos Aires
ARGENTINA

[2]Laboratorio de Bio Toxicología Ambiental,
Instituto de Tecnologías Emergentes y Ciencias Aplicadas (ITECA) UNSAM-CONICET,
25 de Mayo y Francia, B1650 San Martin, Buenos Aires,
ARGENTINA

Abstract: - Airborne particles affect the health of the population. As particles decrease in size, they can penetrate deeper into the respiratory system, reaching the terminal bronchioles and alveoli. Particles as small as 0.1 μm in diameter may translocate into the bloodstream, potentially impacting various organs. Additionally, the smaller the particle size, the longer they remain suspended in the air, thereby increasing their deleterious damages. The aim of this work is to study the size distribution of airborne particles emitted from anthropogenic sources of air pollution, with a special emphasis on estimating the distribution of micro and nanoparticles considered the most harmful to health. The Bidimensional Empirical Mode Decomposition (BEMD) algorithm was used on micrographs of the particles obtained by Scanning Electron Microscopy (SEM). BEMD is a current empirical computational tool applied to image analysis that allows extracting non-linear heterogeneous oscillations of brightness. We studied ROFA (Residual Oil Fly Ash) from industrial sources and DEP (Diesel Exhaust Particles) from vehicular emissions as airborne particles. After collecting the particles on filters, micrographs were taken using SEM at different magnifications to which the BEMD algorithm was applied. Particle size and asymmetry distributions were obtained for each mode, allowing the identification of the most deleterious particles. The methodology employed herein is relatively simple and effective for inferring the impact of airborne particulate matter on health and the environment.

Key-Words: - airborne particles, morphological characterization, Scanning Electron Microscopy (SEM), Bidimensional Empirical Mode Decomposition (BEMD), Generalized Extreme Value Distribution (GEV).

Received: March 26, 2024. Revised: August 27, 2024. Accepted: September 19, 2024. Published: October 21, 2024.

1 Introduction

Proper characterization of bidimensional structures significantly impacts applications, leading to better decisions in assessing pollution consequences. Multiscale methods and algorithms, such as Bidimensional Empirical Mode Decomposition (BEMD), are continuously evolving. Their optimization allows for simpler, more accurate, and precise representation of information. Empirical Mode Decomposition (EMD), introduced by Huang et al. in 1989 [1] for one-dimensional analysis, is effective for non-stationary and nonlinear time series. In 2003, [2], extended EMD to BEMD for image texture analysis, leading to ongoing advancements in BEMD, [3]. The BEMD algorithm is a computational tool that enables the extraction of nonlinear, heterogeneous brightness oscillations from an image. This study focuses on analyzing multimodal images and their decomposition using BEMD, applied to Scanning

Electron Microscopy images of airborne urban dust particles.

Air pollution is a mixture of gasses and suspended Particulate Matter (PM) from both anthropogenic sources [4] and natural events [5]. Urban environments are significantly impacted by airborne dust particles, which pose risks to human health, environmental quality, and urban infrastructure. Epidemiological investigations reveal a correlation between elevated concentrations of PM from different sources and heightened rates of morbidity and mortality associated with cardiopulmonary diseases, as well as an increased incidence of lung cancer, [6], [7], [8]. In 2009, the World Health Organization [9] (WHO, 2009) declared that air pollution was responsible for 8% of lung cancer and 5% of deaths from cardiopulmonary causes in the world. Furthermore, in 2013, the International Agency for Research on Cancer (IARC) classified MP as carcinogenic to humans, [10].

In this context, several *in vitro* and *in vivo* experimental studies have provided conclusive evidence regarding the direct genotoxic effects of airborne PM resulting from its physicochemical characteristics, as well as the indirect genotoxicity observed in response to PM-induced inflammation, [11], [12]. Specifically, concerning the subjects discussed in this article, various authors have consistently demonstrated and continue to elucidate the detrimental impacts of anthropogenic particulate matter derived from urban and industrial sources, such as diesel exhaust particulate matter (DEP) and Residual Oil Fly Ash (ROFA), on human health, [13], [14], [15], [16], [17], [18].

The atmosphere, whether in urban or remote areas, contains significant concentrations of aerosol particles sometimes as high as 10^7-10^8 cm^{-3}. The diameters of these particles span over four orders of magnitude, from a few nanometers to around 100μm. To appreciate this wide size range, one just needs to consider that the mass of a 10μm diameter particle is equivalent to the mass of one billion 10-nm particles. Combustion generated particles, such as those from automobiles, power generation, and woodburning, can be as small as a few nanometers and as large as 1μm. Windblown dust, pollens, plant fragments, and seasalt are generally larger than 1μm. Material produced in the atmosphere by photochemical processes is found mainly in particles smaller than 1μm. The size of these particles affects both their lifetime in the atmosphere and their physical and chemical properties. It is therefore necessary to develop methods to mathematically characterize particle size distributions, [19].

The topic concerning the number size distribution of particles in the range 1-1000 nm is presently under active investigation in current research, e.g. various advanced particle size magnifiers were developed in the last ten decades, [20], [21]. SEM and image processing have been effectively employed in prior studies to assess the morphology, particle size, and particle size distribution of airborne hardwood sanding dust, [22].

The aim of this work is to study the size distribution of airborne particles emitted by anthropogenic sources of pollution, with a special emphasis on estimating the distribution of micro- and nanoparticles, which are considered the most harmful to health.

2 Problem Formulation

To achieve the precision needed for obtaining air particle size distribution and morphological characteristics, advanced techniques such as Scanning Electron Microscopy (SEM) and Bidimensional Empirical Mode Decomposition (BEMD) are used in the initial stage. SEM allows for high-resolution imaging and BEMD offers a refined approach to decompose complex structures into simpler components.

Secondly, another challenge lies in accurately characterizing the size and morphology of airborne urban dust particles to better understand their health impacts. To this end, we need adequate characterization for the location, size and morphology of particles.

3 Materials and Methods

3.1 Particle Sources

Herein, we employed particles from two different sources: Residual Oil Fly Ash (ROFA) and Diesel Exhaust Particles (DEP).

- Residual Oil Fly Ash (ROFA) collected from the Mystic Power Plant, CT, USA, was employed as a recognized surrogate ambient particulate matter and was kindly provided by J.

Godleski (Harvard School of Public Health, Boston, MA, USA).

- Diesel exhaust particles (DEP) (SRM2975) were purchased from the US National Institute of Standards and Technology.

3.2 Scanning Electron Microscopy

Average particle size (APS), size distribution, and morphology of both types of particulate matter, ROFA and DEP, were studied using SEM (Quanta 250 FEISEM, Pantelimon, Romania) coupled to a (ThermoFisher) energy-dispersive X-ray spectroscopy (EDX) detector for chemical composition analysis. For this purpose, the PM particles were attached to a double-sided carbon conductive tape, and loose powder was eliminated using a N_2 gun to avoid the release of particles inside the microscope chamber when starting the vacuum pump or ventilation; the samples were analyzed after coating them with gold by direct current sputtering. Images were obtained using a high-efficiency in-lens detector to achieve clear topographic images in high vacuum mode at an acceleration voltage of 4kV-10kV.

3.3 Algorithm for Particle Characterization

Once the image (matrix) has been decomposed following, [23] into Bidimensional Implicit Mode Functions (BIMFs), the particles or structure elements can be identified by locating the local maximum values within each of these matrices. Subsequently, for every detected particle, its size is determined by assessing the local minimum values along the horizontal (H) and vertical (V) direction from each local maximum. This process yields four values, denoted clockwise as r_1, r_2, r_3, and r_4. Note that, since the particles are randomly oriented, these values are of statistical nature. The particle diameter (d) and asymmetry (A) are defined as:

$$d=2\ \max\{r_1,r_2,r_3,r_4\} \tag{1}$$

$$A=\frac{|dH-dV|}{\max\{dH,dV\}} \tag{2}$$

where

$$dH=r_2+r_4,\quad dV=r_1+r_3 \tag{3}$$

The flowchart of the proposed algorithm that determines and computes particle sizes and asymmetries is presented in Figure 1.

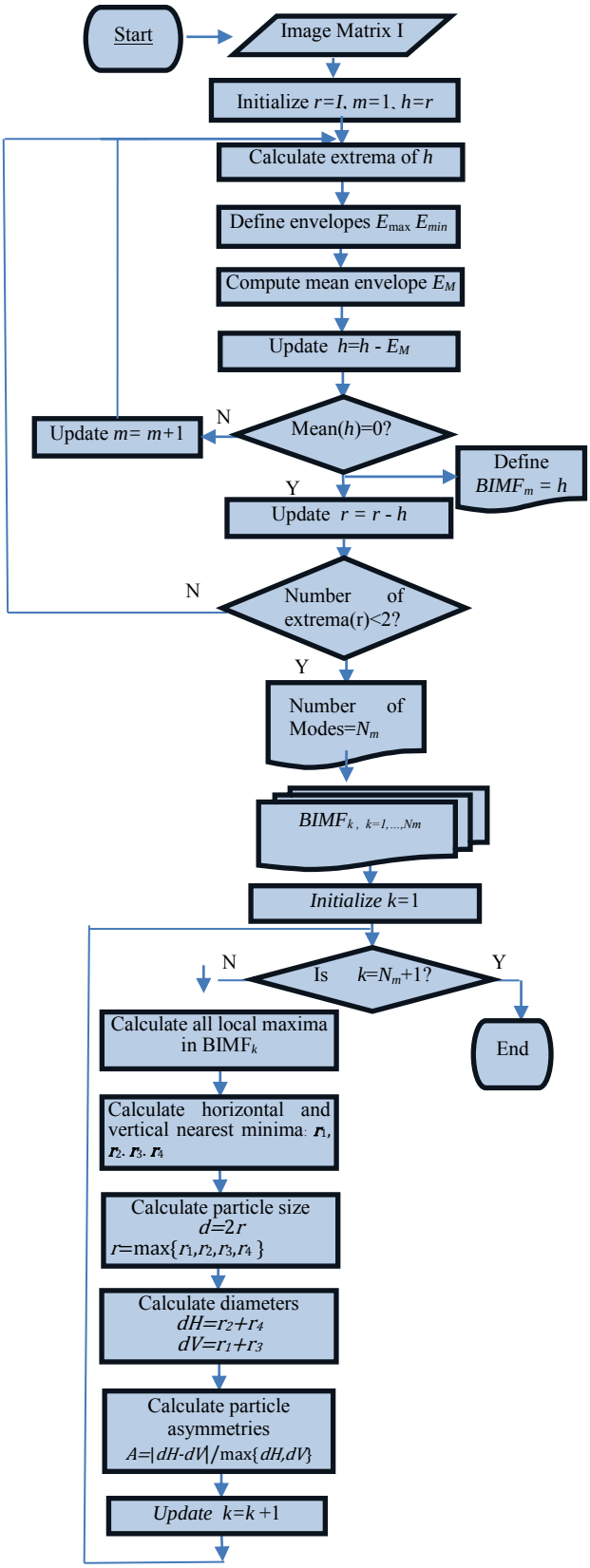

Fig. 1: Flowchart of the proposed algorithm

After applying the algorithm, we proceed to obtain the histogram of the particle sizes for each mode.

Each histogram is fitted by a statistical distribution that is selected according to *qqplot* (quantile-quantile plot) that is a graphical method for comparing two probability distributions by plotting their quantiles against each other.

In the next section, the algorithm is applied to two examples: ROFA and DEP images.

4 Results and Discussion

PM sizes, air particles are conventionally classified as coarse (PM10), fine (PM2.5), and ultrafine (PM0.1) particles, corresponding to their aerodynamic diameters being lower than 10μm, 2.5μm, and 100nm, respectively. Lower diameters imply higher deleterious impact on public health. We show for ROFA and DEP one original SEM image and significant BIMFs images obtained by BEMD in Figure 2 and Figure 3.

Then we select the significant modes for each case and obtain the histogram for particle sizes for these modes. Significant modes are those where the smallest details correspond to individual particles rather than boundaries. In the higher modes, associated with larger structures, enough particles should be detected to obtain a representative distribution. After evaluating various distribution types for fitting the histogram for particle sizes, Generalized Extreme Values (GEV) distribution was selected for both examples, due to its superior performance according to the *qqplot*. The fitting parameters for GEV distribution are:

κ: Shape parameter (type of tail behavior),

σ: Scale parameter (spread or dispersion),

μ: Location parameter (central value).

Section 4.1 is concerned with ROFA particles. Section 4.2 is concerned with DEP particles.

4.1 Example 1: Application to ROFA

By comparing the original ROFA image in Figure 2, it can be observed that BIMF1 and BIMF2 primarily correspond to particle boundaries, while BIMF3 and BIMF4 display structures resembling particles of varying sizes. In contrast, BIMF5 presents a more diffuse image with fewer particles. For this reason, only Modes 3 and 4 are considered significant.

Figure 4 shows a histogram of the particle size distribution along with the fitted GEV distribution for the ROFA significant modes. The estimated GEV parameters are also included in Figure 4 while the confidence intervals are in Table 1. As expected, Mode 3 identified a significant number of the smallest particles. This is highlighted by the location parameter μ (GEV location parameter), which takes a value close to 8μm. Moreover, particle sizes in BIMF3 are more concentrated since the value of spread parameter (GEV parameter σ.) is smaller than BIMF4 and has a shorter tail (related to the GEV parameter κ).

There is not a clear relationship between the degree of asymmetry and the size of a particle. However, the plots of asymmetry versus diameter presented in Figure 5 suggest that the degree of asymmetry of the particles tends to increase with diameter in both Mode 3 and Mode 4.

4.2 Example 2: Application to DEP

In this example, Figure 3 suggests that modes BIMF2, BIMF3 and BIMF4 show structures related to particles having different sizes while BIMF5 shows a more diffuse image with a lower quantity of particles. For this reason, in this case Modes 2, 3 and 4 are considered for analysis.

In Figure 6 and Figure 7 are plotted the results obtained for particle sizes and asymmetries for DEP for each significant mode.

In this case, GEV distribution showed a better performance for fitting the histogram. The estimated parameters for each Mode are included in Figure 6 while the confidence intervals are in Table 2.

Modes 2 and 3 primarily identify ultrafine particles while Mode 4 captures fine particles. It is confirmed that, as usual, both particle size and spread increase with the mode number.

To analyze the degree of symmetry, we plotted asymmetry versus diameter in Figure 7, as it was done for ROFA (Figure 4). In DEP example, the points representing asymmetry versus size for each detected particle are more randomly dispersed.

These findings are important because, as it was mentioned before, the smallest airborne particles significantly impact human health due to their ability to penetrate deep into the respiratory system and enter the bloodstream. Once inside the body, they can cause inflammation, oxidative stress, and cellular damage. Prolonged exposure to ultrafine particles has been linked to a range of adverse health effects, including respiratory and cardiovascular diseases, and even cancer.

a)

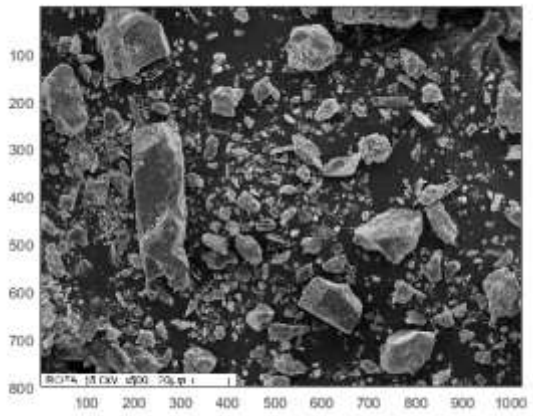

b)

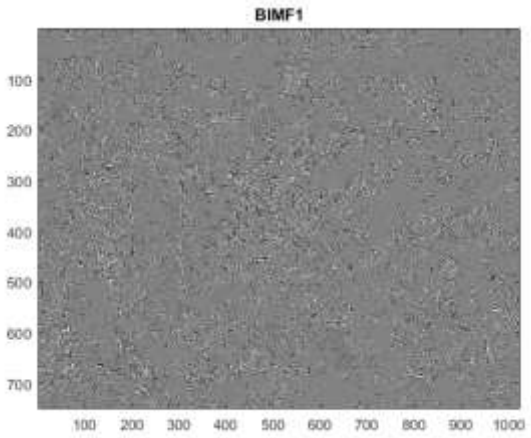

c)

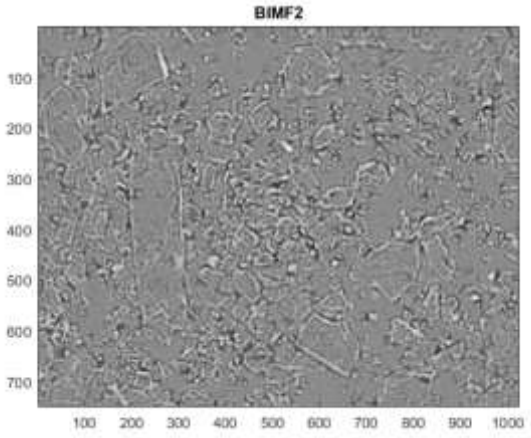

d)

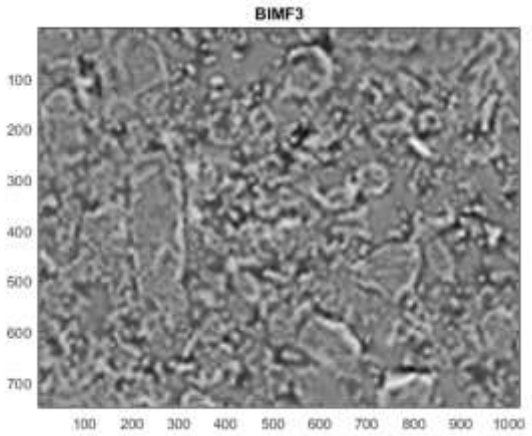

e)

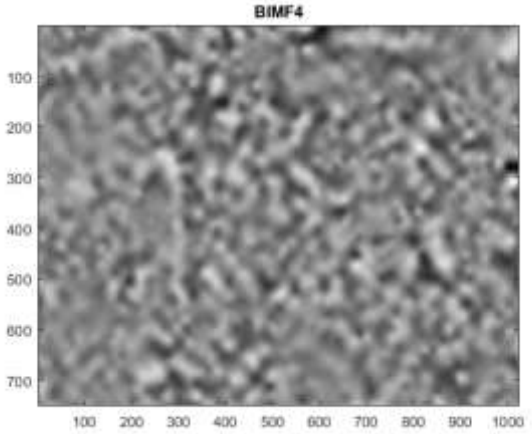

f)

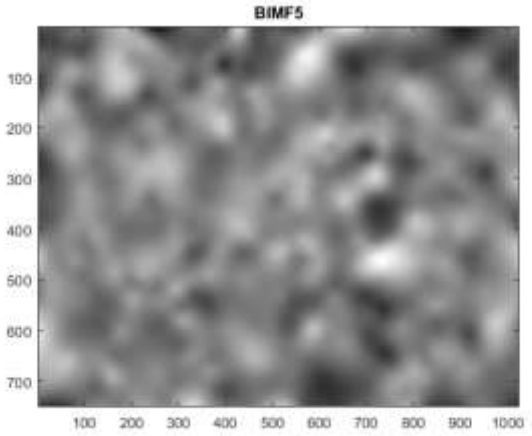

Fig. 2: a) Original ROFA SEM image. b) -f) Successive BEMD Modes BIMF1–BIMF5

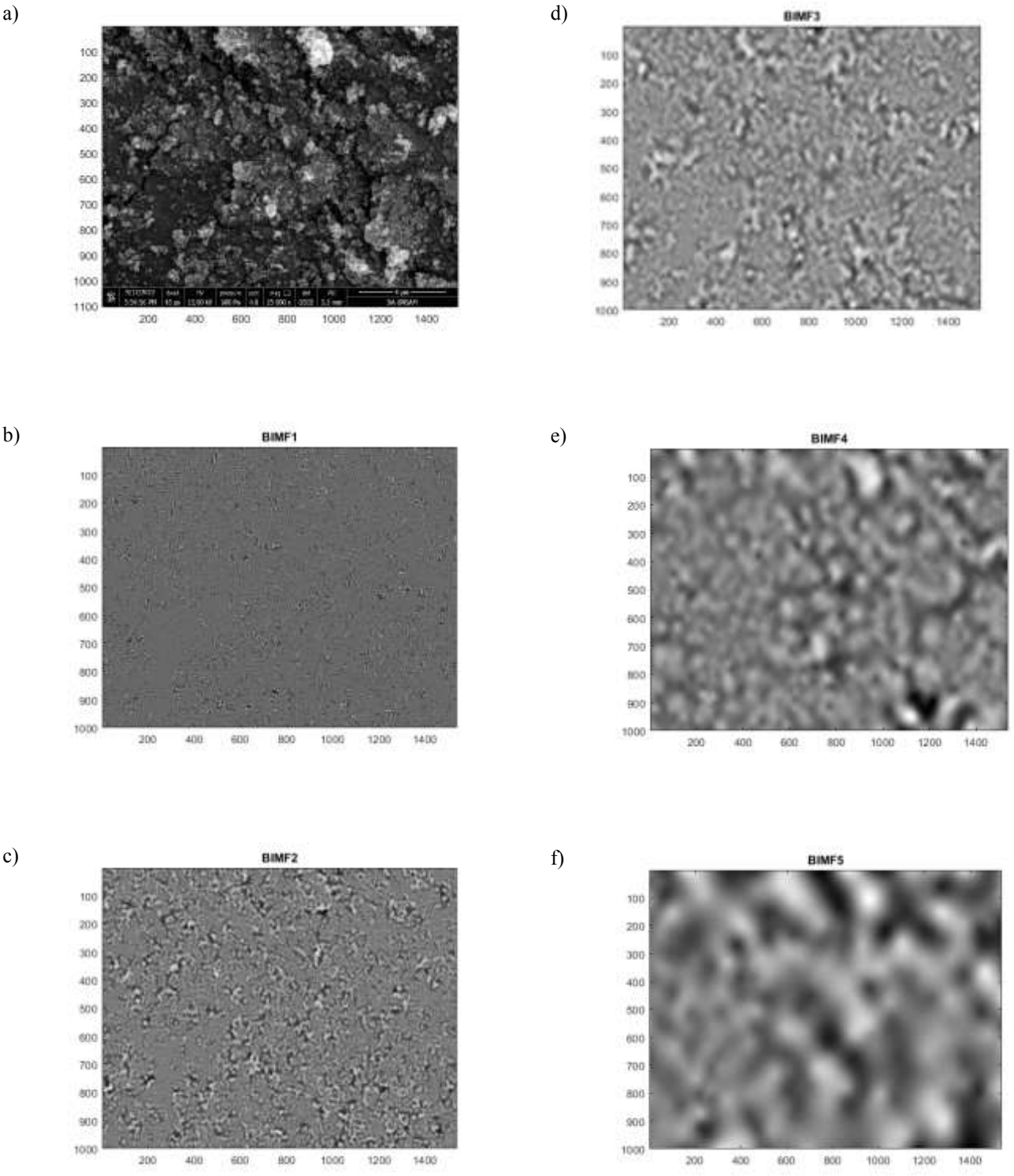

Fig. 3: a) Original DEP SEM image. b)-f) Successive significant BEMD Modes IMF1–IMF5

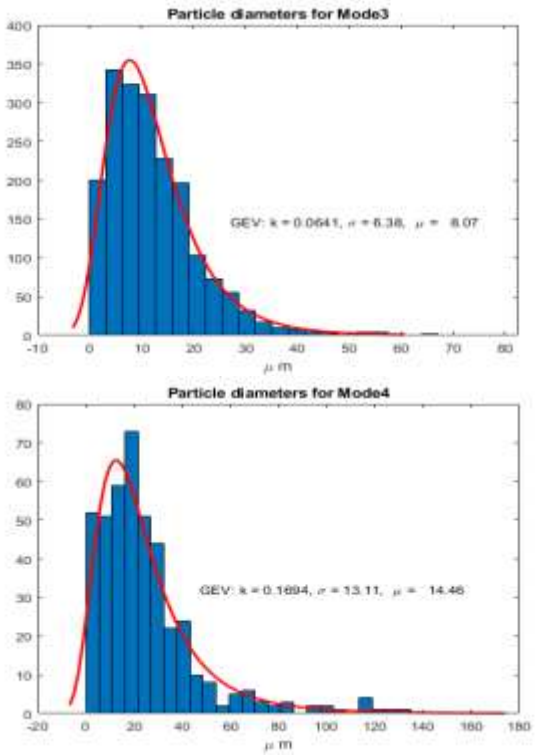

Fig. 4: ROFA particles histogram and GEV fitting distribution for the diameters identified in significant Mode 3 (top) and Mode 4 (bottom)

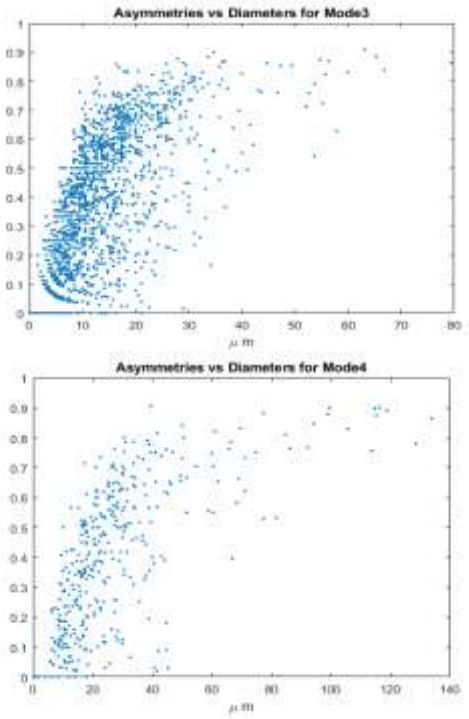

Fig. 5: ROFA particles asymmetries vs. diameters of the identified particles in significant Mode 3 (top) and Mode 4 (bottom)

Table 1. Confidence Intervals for GEV fitting parameters (ROFA)

Mode	κ	σ	μ
3	[0.031, 0.097]	[6.145, 6.624]	[7.754, 8.398]
4	[0.0912 0.247]	[12.06, 14.27]	[13.04,15.875]

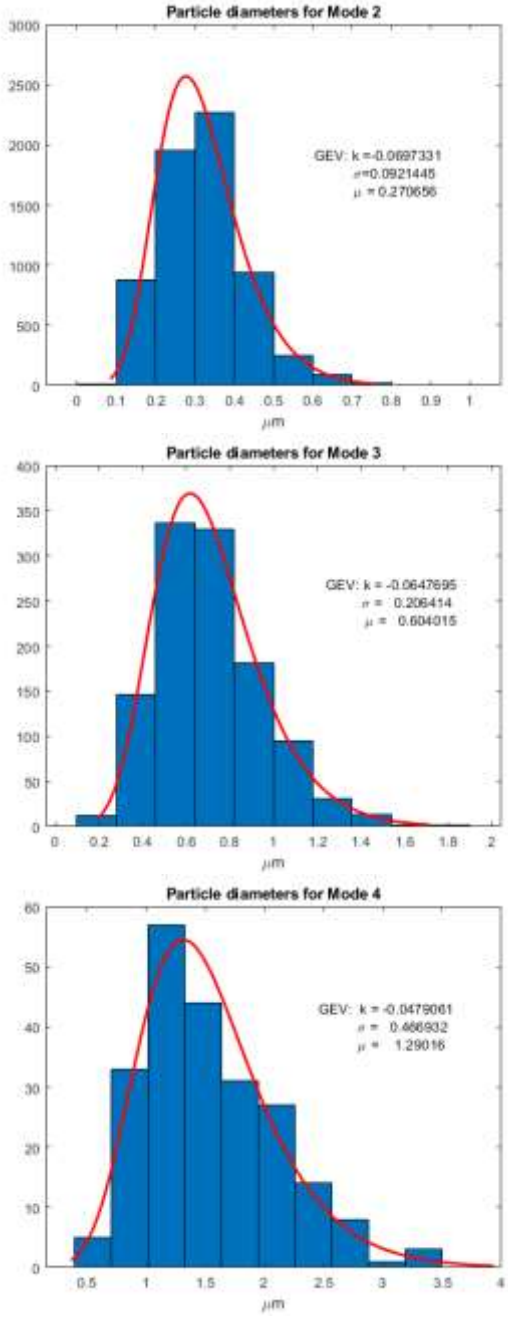

Fig. 6: DEP particles histogram and GEV fitting distribution for the diameters identified in significant IMF: Mode 2 (top), Mode 3 (middle) and Mode 4 (bottom)

Table 2. Confidence Intervals for GEV fitting parameters (DEP)

Mode	κ	σ	μ
2	[-0.085, 0.054]	[-0.10, -0.02]	[-0.152, 0.06]
3	[0.074, 0.178]	[0.197, 0.216]	[0.42, 0.520]
4	[0.268, 0.273]	[0.591, 0.617]	[1.22, 1.36]

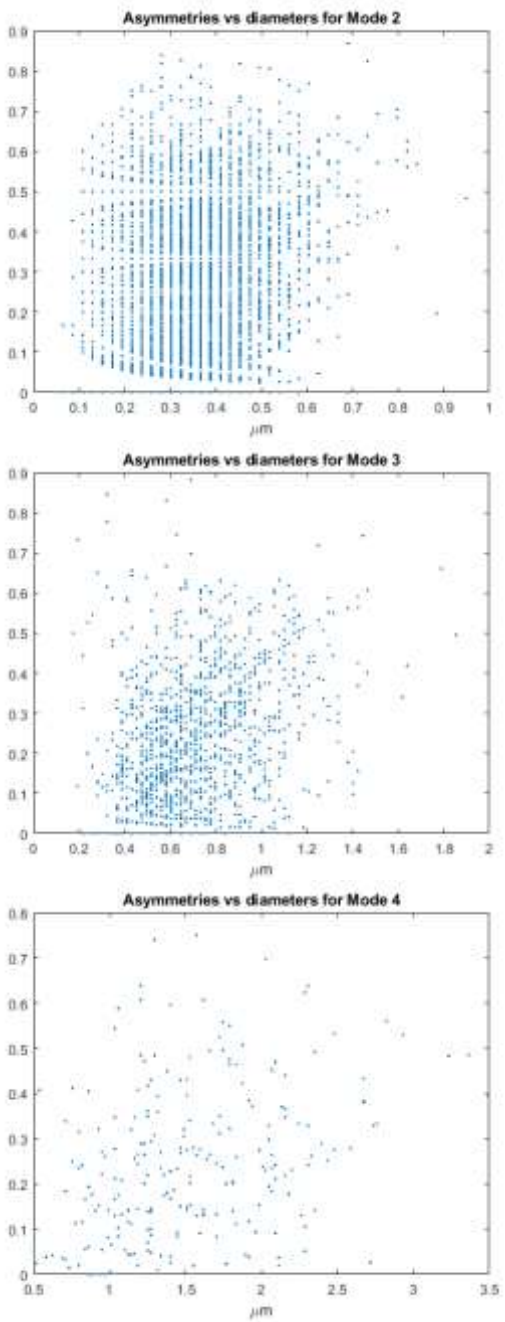

Fig. 7: DEP particles asymmetries versus diameters of the identified particles in Mode 2 (top), Mode 3 (middle) and Mode 4 (bottom)

5 Conclusion

The Bidimensional Empirical Mode Decomposition (BEMD) allowed obtaining the multimodal distribution of airborne dust particle size from scanning electron micrographs. We proposed an algorithm that begins with BEMD. Once the component images are obtained, they are compared with the original image to identify the significant modes. In the applications presented in this work, these modes are associated with particles, with the consideration that enough particles are necessary for statistical size distribution analysis. The algorithm then identifies particles for each significant mode, calculates their sizes, and evaluates their asymmetry. This technique was applied to SEM micrographs of ROFA and DEP particles, providing valuable insights into the morphological features of these airborne particles. The ROFA samples, consisting mainly of microparticles, were distinguished by their irregular shapes and varying sizes, whereas the DEP samples comprised relatively more symmetric nanoparticles, reflecting their different sources and formation processes. For each significant mode, histograms of particle size distribution were appropriately fitted with Generalized Extreme Value (GEV) distributions. This fitting process provided a robust statistical framework to describe the particle populations, highlighting the prevalence of certain size ranges and the variability within the samples.

While further analysis is needed to gather robust information for decision-making, the methodology employed herein is relatively simple and effective for inferring the impact of the different sources of airborne particulate matter on health and the environment.

Declaration of Generative AI and AI-Assisted Technologies in the Writing Process

During the preparation of this work the authors used Grammarly for language editing. After using this service, the authors reviewed and edited the content as needed and take full responsibility for the content of the publication.

References:

[1] Huang, N.E., Shen, Z., Long, S.R., Wu, M.C., Shih, H.H., Zheng, Q., Yen, N, Tung, C.C., Liu, H.H., The Empirical Mode Decomposition and the Hilbert Spectrum for Nonlinear and Non-stationary Time Series Analysis, *Proceedings of the Royal Society of London. Series A: Mathematical, Physical and Engineering Sciences,* Vol. 454, 1998, pp. 903 - 995.

[2] Nunes, J., Bouaoune, Y., Deléchelle, É., Niang, O., Bunel, P., Image Analysis by Bidimensional Empirical Mode Decomposition, *Image Vis. Comput.*, Vol. 21, 2003, pp. 1019-1026.

[3] Xie Q., Hu J., Wang X., Du Y., Qin H., Novel optimization-based bidimensional empirical mode decomposition. *Digital Signal Processing*, Vol. 133, 2023, 103891.

[4] Atkinson, R., Fuller, G., Anderson, H, Harrison, R., Armstrong, B., Urban Ambient Particle Metrics and Health: A Time-series Analysis. *Epidemiology,* Vol. 21, No 4, 2010, pp 501-511.

[5] Horwell, C., Baxter, P. The Respiratory Health Hazards of Volcanic Ash: A Review for Volcanic Risk Mitigation, *Bulletin of Volcanology,* Vol. 69, No 1, 2006, 1-24.

[6] Pope, C., Douglas W., Health Effects of Fine Particulate Air Pollution: Lines That Connect, *Journal of the Air & Waste Management Association*, Vol. 56, No 6, 2006, pp.709–742.

[7] Katanoda, K., Sobue, T., Satoh, H., Tajima, K., Suzuki, T., Nakatsuka, H., Nitta, H., Tanabe, K, and Tominaga, S. An Association Between Long-term Exposure to Ambient Air Pollution and Mortality from Lung Cancer and Respiratory Diseases in Japan, *Journal of epidemiology*, Vol. 21, No 2, 2011, pp. 132-143.

[8] Carey, I. M., Atkinson, R. W., Kent, A. J., Van Staa, T., Cook, D. G., and Anderson, H. R., Mortality Associations with Long-term Exposure to Outdoor Air Pollution in a National English Cohort, *American Journal of Respiratory and Critical Care Medicine*, Vol. 187, No 11, 2013, pp. 1226-1233.

[9] *World Health Statistics 2009*, World Health Organization, 2009, [Online]. https://www.who.int/publications/i/item/9789241563819 (Accessed Date: October 1, 2024).

[10] Loomis, D., Grosse, Y., Lauby-Secretan, B., El Ghissassi, F., Bouvard, V., Benbrahim-Tallaa, L., Guha, N., Baan, R, Mattock, H. and Straif, K.,The Carcinogenicity of Outdoor Air Pollution, *The Lancet,* Vol.14, 2013, pp. 1262-1263.

[11] Schins, R., Mechanisms of Genotoxicity of Particles and Fibers, *Inhalation toxicology*, Vol. 14, No 1, 2002, pp. 57-78.

[12] Wessels, A., Albrecht C., Knaapen A., Duffin, R., Berlo D. van, Voss, P., Unfried, K., Schins, R., Nanoparticle-Induced Inflammation and Its Effect on the Base Excision Repair Pathway in Rat Lungs, *Toxicology Letters*, Vol.172, 2007, pp. S175.

[13] Ceron-Breton, J. G., Ceron-Breton, R. M., Ramirez-Lara, E., Rojas-Dominguez, L., Vadillo-Saenz, M.S., Guzman-Mar, J.L. Measurements of Atmospheric Pollutants (Aromatic Hydrocarbons, O3, NOx, NO, NO2, CO, and SO2) in ambient air of a site located at the northeast of Mexico during summer 2011. *WSEAS Transactions on Systems*, Vol. 12, 2013, p.55-66.

[14] Shuhaili, A., Ihsan, F. A. and Waleed, S., Air Pollution Study of Vehicles Emission in High Volume Traffic: Selangor, Malaysia as a Case Study, *WSEAS Transactions on Systems*, Vol. 12, 2013, p.67-84.

[15] Petrus, M., Popa, C., & Bratu, A. M., Urban Air Pollution by Laser Photoacoustic Spectroscopy and Simplified Numerical Modeling of Gas Pollution in Urban Canyon, *WSEAS Transactions on International Journal of Environmental Engineering and Development,* vol. 2, pp. 99-105, 2024.

[16] Tau. J., Novaes, P., Matsuda, M., Tasat, D., Saldivia, P., Berra, A., Diesel exhaust particles selectively induce both proinflammatory cytokines and mucin production in cornea and conjunctiva human cell lines, *Investigative Ophtalmology and Visual Science,* Vol. 54, 2013, pp. 4759-4765.

[17] Jimoh, Y. A., Lawal, A. O., Kade, I. J., Olatunde, D. M., & Oluwayomi, O., Diphenyl diselenide modulates antioxidant status, inflammatory and redox-sensitive genes in diesel exhaust particle-induced neurotoxicity. *Chemico-Biological Interactions*, *367*, 110196, 2022.

[18] Kurtz, M., Lezón, CH., Masci, I., Boyer. P., Brites, F., Bonetto, J., Bozal, C., Álvarez, L., Tasat, D., Air pollution induces morpho-functional, biochemical and biomechanical vascular dysfunction in undernourished rats, *Food and Chemical Toxicology,* Volume 190, 2024, pp. 114777

[19] Seinfeld, J. H., Pandis, S. N., *Atmospheric Chemistry and Physics: From Air Pollution to Climate Change,* John Wiley & Sons, Inc. (2006)

[20] Zeraati-Rezaei, S., Al-Qahtani, Y., Herreros, J. M., Ma, X., and Xu, H. Experimental investigation of particle emissions from a Dieseline fuelled compression ignition engine. *Fuel*, Vol. 251, pp. 175-186.

[21] Lehtipalo, K., Ahonen, L., Baalbaki, R., Sulo, J., Chan, T., Laurila, T., Dada, L., Duplissy, J., and Vanhanen, J., The standard operating procedure for Airmodus Particle Size Magnifier and nano-Condensation Nucleus Counter. *Journal of Aerosol Science*, Vol. 156, 2021, pp.105822.

[22] Mazzoli, A., Favoni, O., Particle size, size distribution and morphological evaluation of airborne dust particles of diverse woods by scanning electron microscopy and image processing program, *Powder Technology*, Vol. 225, 2012, pp. 65-71.

[23] Sasikanth. Bidimensional Empirical Mode Decomposition (BEMD), MATLAB Central File Exchange. Retrieved April 19, 2023.

Contribution of Individual Authors to the Creation of a Scientific Article (Ghostwriting Policy)

The authors contributed equally to this research, participating in all stages from problem formulation to final findings, solutions and writing. M. Morvidone, D. Rubio and R. Piotrkowski. were engaged in the mathematical and computations formulation and the algorithm development and writing. I. Masci, M. Kurtz and D. Tasat in the biological formulation, the SEM images and writing.

Sources of Funding for Research Presented in a Scientific Article or Scientific Article Itself

This work is part of the Scientific and Technological Research Project (PICT 2021-I-A-00598)

Conflict of Interest

The authors have no conflicts of interest to declare.